A novel ^{18}F-labeled PSMA ligand for PET/CT imaging of prostate cancer patients: First -in-man observational study and clinical experience with ^{18}F-JK-PSMA-7 during the first year of application

Brief title: ^{18}F-JK-PSMA-7 in prostate cancer patients

Felix Dietlein[1,2], Melanie Hohberg[1], Carsten Kobe[1], Boris D. Zlatopolskiy[3], Philipp Krapf[4], Heike Endepols[1,3], Philipp Täger[1], Jochen Hammes[1], Axel Heidenreich[5], Bernd Neumaier[3,4*], Alexander Drzezga[1*] and Markus Dietlein[1*§]

[1] Department of Nuclear Medicine, University Hospital of Cologne, Germany

[2] Department of Medical Oncology, Dana-Farber Cancer Institute, Harvard Medical School, Boston, USA

[3] Institute of Radiochemistry and Experimental Molecular Imaging, University Hospital of Cologne, Germany

[4] Institute of Neuroscience and Medicine, INM-5: Nuclear Chemistry, Forschungszentrum Jülich GmbH, Germany

[5] Department of Urology, University Hospital of Cologne, Germany

* B.N. and A.D. and M.D. contributed equally to this work.

§ **Corresponding author:** Markus Dietlein, Department of Nuclear Medicine, University Hospital of Cologne, Kerpener Str. 62, 50937 Cologne, Germany. Email: markus.dietlein@uk-koeln.de, Tel.: +49 221 478 5024, Fax: +49 221 478 89085

ABSTRACT

In preclinical trials, the recently developed tracer ^{18}F-JK-PSMA-7 (2-MeO-^{18}F-DCFPyL) has been demonstrated to show favorable properties regarding clinical performance and radiochemical accessibility. The aim of this study was to evaluate the clinical utility of ^{18}F-JK-PSMA-7 for PET/CT imaging of patients with prostate cancer.

Methods: In an Institutional Review Board-approved pilot study, initial clinical utility of PET/CT imaging with ^{18}F-JK-PSMA-7 was directly compared to ^{68}Ga-PSMA-11 PET/CT in a group of 10 patients with prostate cancer. The two PSMA-tracers were administered in each patient less than 3 weeks apart. Next, we analyzed the data of 75 consecutive patients who had undergone clinical ^{18}F-JK-PSMA-7 PET/CT imaging for tumor localization of biochemical recurrence (BCR).

Results: The pilot study in 10 patients who were examined with both PSMA-tracers demonstrated that ^{18}F-JK-PSMA-7 was at least equivalent to ^{68}Ga-PSMA-11. Using ^{18}F-JK-PSMA-7, all unequivocally ^{68}Ga-PSMA-11 positive lesions could be also detected by PET/CT and in 4 patients additional suspicious PSMA-positive lesions were identified (one patient changed from PSMA-negative to PSMA-positive). In patients with BCR (after prostatectomy or radiotherapy), the capacity of ^{18}F-JK-PSMA-7 PET/CT to detect any PSMA-positive lesions was 84.8%. The PSA-stratified detection rate of ^{18}F-JK-PSMA-7 after prostatectomy varied between 54.5% (6/11 patients; PSA < 0.5µg/l), 87.5% (14/16 patients; PSA 0.5-2 µg/l) and 90.9% (20/22 patients; PSA > 2µg/l).

Conclusion: The tracer ^{18}F-JK-PSMA-7 was found to be safe and clinically useful. We demonstrated that ^{18}F-JK-PSMA-7 was not inferior, when directly compared with ^{68}Ga-PSMA-11 in a pilot study but indeed identified additional PSMA-avid suspicious lesions in oligo-metastasized patients with BCR. In a subsequent analysis of a clinical cohort of BCR patients, ^{18}F-JK-PSMA-7 was useful in tumor localization. ^{18}F-JK-PSMA-7 is recommended for future prospective trials.

INTRODUCTION

When a patient experiences a new increase of PSA levels after surgery or radiation therapy of prostate cancer, commonly referred to as a biochemical recurrence (BCR), sensitive imaging modalities are needed to decide on metastasis-directed therapy (MTD) options (*1,2*). Over the past years, radio-labeled PSMA specific PET tracers have been increasingly used to localize prostate cancer (*3-9*). The rationale behind these tracers is the fact that tumor cells display an ∼8-12-fold increased expression of folate hydrolase 1, better known as prostate-specific membrane antigen (PSMA) on their surface, compared with noncancerous prostate tissue *(10-11)*. An additional advantage of PSMA specific PET tracers is that they are not negatively effected by therapies targeting the signaling of the androgen receptor in castration-resistant prostate cancer (*12*).

Most PET tracers currently established for cancer detection are labeled with ^{18}F, due to their ideal decay properties regarding half-life, availability at a cyclotron, and its high image resolution, due to its low β+-emission energy (*13,14*). However, regarding PSMA-ligands, ^{68}Ga-labeled compounds were the first widely used in clinical studies (*15*). Advantages are that no access to a cyclotron is required and that ^{68}Ga-labeled tracers can be easily obtained without complex radiosynthetic chemistry, since the ^{68}Ga label can be introduced by simple complex formation with an appropriate chelator (*16*). In 2011, Chen and colleagues reported on the ^{18}F-labeled PSMA specific tracer ^{18}F-DCFPyL, by using a multistep synthesis protocol, which involved the radiofluorination of a prosthetic group (*17*). Clinical studies revealed that ^{18}F-DCFPyL displayed at least non-inferior sensitivity in detecting relapsed tumors in prostate cancer patients, compared with ^{68}Ga-PSMA-11 (*6,7,18,19*). In some patients, these tracers even exhibited increased sensitivity, possibly due to the increased resolution of the ^{18}F-label for small anatomic structures such as small iliac lymph nodes.

When ^{18}F-labeld PSMA ligands were introduced into the clinical setting, the synthesis of ^{18}F-labeled PSMA was far more difficult than the preparation of their ^{68}Ga-labeled counterparts in routine clinical practice (*17,20*). Indeed, if the synthesis reaction of ^{18}F-DCFPyL is not performed under optimal conditions, an unstable isomer is formed, which leads to rapid defluorination of the ^{18}F-labeld PSMA specific product (*21,22*).

Recently, our group introduced the novel PSMA specific derivative 2-MeO-^{18}F-DCFPyL (^{18}F-JK-PSMA-7), a new compound for PSMA specific PET imaging. This compound had been selected from a group of several candidates due to its favorable imaging properties (*23*). The abbreviation JK (J = Jülich; K = Köln) refers to the Forschungszentrum Jülich and the University Hospital of Cologne which were involved in the development of this novel tracer. In addition, we recently reported on a "minimalist" approach for the synthesis of ^{18}F-JK-PSMA-7. This enabled to implement a robust and high yielding synthesis process with minor variations in release specifications ideally suited for high-throughput productions in a clinical setting. (*23*).

Here, we present the first application of ^{18}F-JK-PSMA-7 in a pilot study, demonstrating its non-inferiority as compared to the benchmark tracer ^{68}Ga-PSMA-11. Furthermore, we report the results of the first routine clinical application of this tracer in a cohort of 75 prostate cancer patients with biochemical recurrence (BCR).

MATERIALS AND METHODS

Study design and patient selection criteria

In brief, our study followed a two-step approach. In the first step, we offered 10 patients, who had undergone ^{68}Ga-PSMA-11 imaging, an additional ^{18}F-JK-PSMA-7 PET/CT scan. Nine of these 10 patients had recently experienced a biochemical recurrence (BCR) of their disease, and one patient with known oligometastatic status showed a raised PSA-level. The ^{68}Ga-PSMA-11 scans were interpreted as negative or inconclusive in 5 patients, only one solitary PSMA-lesion has been detected in the other 5 patients. To improve the certainty of the assumed tumor localization or to exclude any additional PSMA-positive metastases, we performed a second PET/CT scan with ^{18}F-JK-PSMA-7 within 3 weeks of the first ^{68}Ga-PSMA-11 scan. The rationale for this was our previous experience indicating potentially superior detection rate of ^{18}F-labeled PSMA specific PET-tracers (*7,18*). We did not observe any adverse side-effects in any of those 10 patients during the entire examination procedure (up to 3 hours after injection of ^{18}F-JK-PSMA-7). Furthermore, in telephone counseling on therapeutic options some weeks later, none of the patients reported any new side-effects.

In the second step, we used the novel ^{18}F-JK-PSMA-7 tracer to examine a cohort of 75 prostate cancer patients with BCR, who were referred to our institute for PET/CT imaging between March 2017 and December 2017 with the following history:
- 49 patients presented with BCR after surgery; 47 of these patients revealed a PSA level of ≥ 0.2 µg/l after nadir.
- 26 patients presented with BCR after radiotherapy (external beam radiation therapy, brachytherapy, seed implantation); 17 of these patients revealed a PSA level of ≥ 2 µg/l above the PSA nadir; 9 patients had an increase of the PSA level of < 2 µg/l and did not fulfill the Phoenix criteria defining the BCR, but nevertheless were referred to restaging due to continuously rising PSA values without any signs of intraprostatic inflammation.

The institutional review board approved this retrospective study and all subjects signed a written informed consent. All procedures were performed in compliance with the regulations of the responsible local authorities (District Administration of Cologne, Germany).

Imaging

Patients fasted for approximately 4 hours before the PET/CT to allow administration of contrast agent when neither CT scans nor MRI scans had been performed previously and to exclude any interference with the novel ^{18}F-JK-PSMA-7. Data on ^{18}F-DCFPyL had previously shown that fasting did not influence PSMA accumulation in metastases (*24*), but we had no data on the influence of fasting on ^{18}F-JK-PSMA-7 uptake. In our pilot study a mean dosage of 141±30 MBq ^{68}Ga-PSMA-11 and a mean dosage of 358±15 MBq ^{18}F-JK-PSMA-7 were injected. Following previously published protocols, ^{68}Ga-PSMA-11 PET scans were acquired one hour after injection (*3-5*). In patients with PSA below 2.0µg/L, a second scan of the pelvis and the lower abdomen was carried out 3 hours after injection, to guarantee maximal sensitivity of the ^{68}Ga-PSMA-11 tracer (*25-28*). In parallel to previous studies using ^{18}F-DCFPyL (*6,7*), ^{18}F-JK-PSMA-7 PET scans were acquired two hours after

tracer injection. In the pilot study, we additionally generated a series of PET-data between 10 and 230 minutes after injection in 9 of our 10 patients, to define the scans with the best visualization of the PSMA-positive tissue (*29*). All images were acquired on a Biograph mCT 128 Flow PET/CT scanner (Siemens Healthineers, Erlangen, Germany). The same filters and acquisition times (15 minutes from the top of the skull to mid-thigh) were used for ^{68}Ga-PSMA-11 one hour after the injection and for ^{18}F-JK-PSMA-7. The second ^{68}Ga-PSMA-11 PET scan had a flow motion bed speed of 0.7 mm/sec instead of 1.5 mm/sec to compensate for the decay of ^{68}Ga-PSMA-11. Non-contrast-enhanced (low-dose) CT scans were conducted in parallel to PET imaging. Images were reconstructed using an ultra-high definition algorithm (*13*).

All PET scans were analyzed by a team of at least two specialists in nuclear medicine and one radiologist. A scan was scored as positive, if focal tracer accumulation was detected in the prostate fossa, in a lymph node or at a distant site. A focal tracer accumulation was interpreted as suspicious lymph node if it showed a morphological correlate on the corresponding CT scan consistent with a regional lymph node, even when the diameter was < 8 mm. The PET/CT reading was performed according to the published criteria for harmonization of the PSMA-PET/CT interpretation (*30,31*).

Tracer preparation

All tracer were produced in accordance with applicable good manufacturing practice (GMP) using a two-step synthesis protocol. Additionally extensive quality control measures, including radiochemical purity, endotoxin testing, pH-value, and the determination of residual content of solvents like acetonitrile, acetone, tertiary butanol, and tetra-ethyl-ammonium-hydrogen-carbonate [TEAHC] were carried out.

In brief, ^{18}F-JK-PSMA-7 was prepared using a two-step reaction: In a first step, the radiolabeled active ester was produced by the nucleophile reaction of ^{18}F with 2-methoxy-N,N,N-trimethyl-5-((2,3,5,6-tetrafluoro-phenoxy) carbonyl) pyridine-2-aminium-trifluoromethanesulfonate (TFP-OMe-OFT) to generate the ester 2,3,5,6-tetrafluorophenyl-6-([18]fluoro)-4-methoxy-nicotinate ([18]FPy-OMe-TFP). In the second step, 4.6 ± 0.1 mg ((S)-5-amino-1-carboxypentyl)-carbamoyl)-L-glutamic-acid (LYS-GLU) was added to [18]FPy-OMe-TFP and subsequently incubated at 45°C for 6 minutes. Then, the final product ^{18}F-JK-PSMA-7 was purified by SPE (OASIS HLB) and formulated in saline. This reaction provided ^{18}F-JK-PSMA-7 in high radiochemical yield up to 40% and a high radiochemical purity (> 95%). The specific concentration of F-PSMA-7 was ≤ 10 µg/ml. The upper limit of the injected volume was 10 ml; the activity of ^{18}F-JK-PSMA-7 was ≥ 30 MBq/ml. Each week, we produced two batches of ^{18}F-JK-PSMA-7. The detailed procedure for the radiosynthesis using the "minimalist light" protocol is described elsewhere (*23*). The activity produced and the radiochemical purity were analyzed for the 74 consecutive batches of ^{18}F-JK-PSMA-7 synthesized within the first year of clinical application.

Synthesis of ^{68}Ga-PSMA-11 was performed as described previously (*32,33*).

RESULTS

Robustness and reliability of ^{18}F-JK-PSMA-7 production

We analyzed the quality of 74 consecutive synthesis batches of ^{18}F-JK-PSMA-7 over the course of 12 months. We found a high radiochemical activity per synthesis (mean activity: 6,660 MBq ± 2,869 MBq; interquartile range 2,712 MBq) and a high radiochemical purity (mean purity: 98.6% ± 1.6%; interquartile range 2.4%). In the course of this study, only 2 out of 74 syntheses (2.7%) failed to reach a radiochemical purity of more than 95%.

Direct comparison between the biodistribution patterns of ^{18}F-JK-PSMA-7 and ^{68}Ga-PSMA-11

We next assessed the validity of the novel tracer ^{18}F-JK-PSMA-7. For this purpose, we offered 10 patients who had just undergone PET/CT imaging with ^{68}Ga-PSMA-11 an additional PET/CT scan with ^{18}F-JK-PSMA-7. We performed the second PET/CT scan within less than 3 weeks and found that all unequivocally ^{68}Ga-PSMA-11-positive lesions could be validated using ^{18}F-JK-PSMA-7. Moreover, 4 patients displayed at least one additional suspicious PSMA-positive lesion on the ^{18}F-JK-PSMA-7 scan, which had been missed by ^{68}Ga-PSMA-11 (Figs. 1-4). Intriguingly, in 3 of these 4 patients the additional PSMA-positive lesions were located in loco-regional lymph nodes (iliac lymph nodes: patients no. 2 and no. 4; retroperitoneal lymph nodes: patient no. 7). In one patient (patient no. 1), a PSMA-positive bone lesion was revealed by ^{18}F-JK-PSMA-7, which was known from the ^{18}F-DCFPyL PET/CT scan 2 years before.

The follow-up data of the 10 patients are summarized in table 1. First, we report the details of the 4 patients with the different PET-findings. In one of these patients (patient no. 4) the first PET/CT scan with ^{68}Ga-PSMA-11 PET/CT was interpreted as completely negative. The PSMA-positive left iliac lymph node, which was detected by ^{18}F-JK-PSMA-7, was a plausible explanation for the BCR in patient no. 4 with a PSA-level of 1.1 ng/ml and was finally confirmed by the tumor growth visible in an externally performed ^{68}Ga-PSMA-11 PET/CT 8 months later. The salvage lymphadenectomy initially undertaken could not verify the PET finding. The PSMA-positive lymph nodes found additionally by the ^{18}F-JK-PSMA-7 scan in two other patients (patient no. 2 and patient no. 7) were localized in the same lymph node area, in which the ^{68}Ga-PSMA-11 PET/CT had already depicted one PSMA-positive lymph node. Both patients received radiotherapy of the PSMA-positive lymph node area and the PSA-level dropped after the irradiation.

Second, we observed concordant findings using both PSMA-tracers in 6 patients: concordantly positive in 2 patients (patients no. 5 and no. 11) and concordantly negative in 4 patients (patients no. 3, no. 7, no. 9 and no. 10). Both PSMA-positive patients showed PSMA-positive tissue within the prostate fossa und received salvage radiotherapy. One out of the 4 PSMA-negative patients was subjected to salvage radiotherapy of the prostate fossa.

Benchmarking the detection rate of ^{18}F-JK-PSMA-7 across 75 prostate cancer patients with BCR

Closing the pilot study, we examined 162 prostate cancer patients with ^{18}F-JK-PSMA-7 (349±53 MBq) within a year of the clinical application of ^{18}F-JK-PSMA-7. Focusing on the localization of BCR as the main indication for PET/CT, we studied the detection rate of ^{18}F-JK-PSMA-7 (347±56 MBq) in 75 patients, aged 69.2±8.1 years, with increasing PSA levels after initial curative treatment, for which it was unclear whether they carried PSMA-positive lesions or not (Table 2). These patients did not receive androgen deprivation therapy. We analyzed the detection rate separately for patients after prostatectomy ± salvage radiotherapy versus patients after radiotherapy alone.

Overall, 49 patients in our study cohort had recently experienced a biochemical recurrence (BCR) after prostatectomy ± salvage radiotherapy. In 40 of these prostatectomy patients, we detected ^{18}F-JK-PSMA-7-positive lesions, resulting in a detection rate of 81.6%. The PSA-stratified detection rate of ^{18}F-JK-PSMA-7 varied between 54.5% (6/11 patients; PSA < 0.5μg/l), 87.5% (14/16 patients; PSA 0.5-2 μg/l) and 90.9% (20/22 patients; PSA > 2μg/l).

Our cohort contained a further group of 26 patients, who presented with a PSA increase after radiotherapy. The detection rate of the ^{18}F-JK-PSMA-7 tracer was 94.1% (16/17) in patients with a BCR according to the Phoenix criteria (PSA levels ≥ 2.0μg/l above the nadir). Some patients were referred to PSMA PET/CT when the PSA increase was repeatedly confirmed but lay below 2.0μg/l and the Phoenix criteria defining the BCR had not yet been reached. In this constellation, the ^{18}F-JK-PSMA-7 PET scan detected PSMA-positive tissue in 33.3% of patients (3/9).

Tumor relapse patterns substantially differed between BCR patients after surgery and radiotherapy. While 19 of the 49 prostatectomy patients (38.8%) displayed PSMA-positivity exclusively in lymph nodes, this pattern was rarely observed in the patients with a PSA increase after radiotherapy (3/26, 11.5%). Several of the radiotherapy patients, however, displayed PSMA-positive tissue exclusively within the prostate (8/26, 30.8%).

Verification

After the introduction of ^{18}F-JK-PSMA-7 into our clinical care procedures, the collection of data on verification became part of our quality assurance program. After an interval of 6 – 18 months we read all the written reports, which were sent to our institute. Additionally, we checked all our electronic patient files.

The PSMA-positive lesions in the 59 patients, who underwent PET/CT for BCR, were confirmed by histology in 6 patients, by follow-up in 17 patients and by morphological imaging in 20 patients. Further information was missing in 16 patients. The histological verification resulted from salvage-lymphadenectomies with PSMA-positive lymph node metastases. The verification by follow-up was based on a decrease in PSA level after radiotherapy (n=9) or the progression of the PSMA-positive lesion after watchful waiting (n=7) or the regression of the PSMA-positive lesion after starting ADT (n=1). One of these patients with progressive PSMA-positive nodal disease on a second PET had shown a positive ^{18}F-JK-PSMA-7 PET/CT, but then negative histology (0/14 lymph nodes) after S-LAD. We therefore did not interpret this ^{18}F-JK-PSMA-7 PET/CT as false-positive. The

verification by morphological imaging summarized patients in whom the CT demonstrated an osteosclerotic or osteolytic lesion (n=11) or a suspicious lymph node ≥ 8 mm within the pelvis (n=7) or a suspicious pulmonary lesion (n=1) or those in whom the MRI had revealed a suspicious lesion within the prostate (n=1).

DISCUSSION

Over the past 4 years, we have successfully introduced ^{18}F-DCFPyL and later ^{18}F-JK-PSMA-7 into our routine PET/CT imaging procedure for prostate cancer patients (*7,18,34*). Zlatopolskiy and co-workers had described the synthesis of ^{18}F-JK-PSMA-7 and we found that production of ^{18}F-JK-PSMA-7 could be produced with a consistently high radiochemical yield and purity (*23*). The robust synthesis of ^{18}F-JK-PSMA-7 substantially reduced the need to reschedule appointments at short notice in our institute. Furthermore, recent preclinical data have highlighted favorable properties of ^{18}F-JK-PSMA-7 in comparison with other ^{18}F-labeled PSMA tracers, e.g. highest edge contrast, resolution, and signal-to-noise-ratio (*23*).

Here we present the first clinical study with ^{18}F-JK-PSMA-7 across 10+75 patients. As a first step, we show that distribution patterns of ^{18}F-JK-PSMA-7 and ^{68}Ga-PSMA-11 are highly concordant in patients consecutively examined with the two tracers. Interestingly, ^{18}F-JK-PSMA-7 increased the detection rate of suspicious lesions in small anatomic structures, such as iliac or retroperitoneal lymph nodes. These lesions might have remained masked by the limited resolution of the ^{68}Ga-emitting tracers, but had a substantial impact on subsequent therapy in some of these patients. This finding corroborates our earlier observations on ^{18}F-DCFPyL (*7,18*). In contrast to our previous studies, however, we were able to observe this improved sensitivity pattern of ^{18}F-JK-PSMA-7, although the acquisition protocol of ^{68}Ga-PSMA-11 had been amended by a second PET scan, 3 hours after injection for patients with PSA levels below 2.0 µg/l (*25-28*). This finding suggests that the ability of ^{18}F-PSMA specific ligands to visualize small anatomic structures reflects an intrinsic quality of the ^{18}F-label and does not result from differences in image acquisition protocols. It remains an intrinsic advantage of the ^{18}F-labeled PSMA ligands that batches with high ^{18}F-activity were produced and that on each application, the ^{18}F-activity injected was higher than the corresponding amount of ^{68}Ga-activity.

As a second step, we measured and compared the detection rate of ^{18}F-JK-PSMA-7 across a cohort of 75 patients with BCR and confirmed that ^{18}F-JK-PSMA-7 tracer sensitivity and metastatic pattern also depended largely on the PSA level and type of previous therapy (surgery vs. radiotherapy). The PSA-stratified detection rates, which we found for ^{18}F-JK-PSMA-7 in this study, were highly concordant with results reported for ^{68}Ga-PSMA-11 by independent institutes with very high expertise in this field (*4*). These observations suggest that the potential sensitivity of the new ^{18}F-JK-PSMA-7 tracer is at least not inferior to previous PSMA tracers. Further, when combining the detection rate of ^{18}F-JK-PSMA-7 across all BCR patients and excluding the patient subgroup with a PSA increase below the Phoenix criteria, we obtained a pooled localization rate of 84.8% (56/66 patients). It should be noted that at the same institute and with the same PET-scanner, but in another cohort with the same patient characteristics, we had observed a pooled localization rate of

79.1% (102/129 patients) for ^{68}Ga-PSMA-11 and of 74.2% (46/62 patients) for ^{18}F-DCFPyL in 2015 (*18*). Indeed, as shown by Mannweiler et al. in immunohistochemical analyses (*35*), lack of PSMA expression intrinsically limits the sensitivity of PSMA tracers to ~84%, so that ^{18}F-JK-PSMA-7 exploits the full sensitivity potential of PSMA tracers.

Dosimetric data on ^{18}F-JK-PSMA-7 were based on animal studies (*23*) and then on a cohort of 10 patients (*29*). ^{18}F-JK-PSMA-7 showed fast excretion via the blood and the kidneys in humans, similar to that seen with ^{18}F-DCFPyL. The blood protein binding of ^{18}F-JK-PSMA-7 was significantly lower compared to ^{18}F-PSMA-1007 and ^{68}Ga-PSMA-11 in animal studies (*23*). The PSMA-positive metastases in patients showed an increase in SUV_{max} and SUV_{peak} up to 3 hours after the injection of ^{18}F-JK-PSMA-7 (*29*).

Limitations: Our head-to-head comparison between ^{68}Ga-PSMA-11 and ^{18}F-JK-PSMA-7 was not designed as a prospective trial. The ^{18}F-JK-PSMA-7 PET scans were clinically indicated due to an equivocal or negative interpretation of the first PET scan with ^{68}Ga-PSMA-11 or due to an oligometastatic status before radiotherapy. It might be possible that the diagnostic accuracy of ^{68}Ga-PSMA-11 PET/CT is underestimated in the initial cohort of 10 patients. Our working group did not set out to conduct the first-in-man observational study based on animal studies (*23*) with testing of ^{18}F-JK-PSMA-7 on healthy volunteers. It is a general advantage of all ^{18}F-labeled PSMA ligands that the injected activities are usually higher than the injected activities of the ^{68}Ga-labeled PSMA ligands. In our pilot study we injected an activity of approximately 2 MBq ^{68}Ga-PSMA-11 per kg body weight, which complies with the recommended range of ^{68}Ga-PSMA (1.8-2.2 MBq per kg body weight) in the international guidelines (*36*), but higher activities of ^{68}Ga-PSMA-11 will have a positive impact on lesion detectability (*37*).

CONCLUSION

We have shown that ^{18}F-JK-PSMA-7 is safe and displays non-inferior sensitivity in prostate cancer patients, compared to ^{68}Ga-PSMA-11. Further, in parallel to previous studies with ^{18}F-DCFPyL, we observed even improved sensitivity of ^{18}F-JK-PSMA-7, a modified version of ^{18}F-DCFPyL, compared to ^{68}Ga-PSMA-11 in a few selected patients with PSMA-positive lesions in small lymph nodes. Additionally the simplicity of ^{18}F-JK-PSMA-7 production implying high radiochemical yields and a robustness propose this PSMA specific agent for routine clinical diagnostics.

DISCLOSURE

B.N., P.K., BD.Z., and A.D. have applied for a patent on ^{18}F-JK-PSMA-7. No other potential conflicts of interest relevant to this article exist.

KEY POINTS:

QUESTIONS: Is ^{18}F-JK-PSMA-7, a modified version of ^{18}F-DCFPyL (2-MeO-^{18}F-DCFPyL), helpful for PET/CT imaging of patients with prostate cancer?

PERTINENT FINDINGS: ^{18}F-JK-PSMA-7 was directly compared to ^{68}Ga-PSMA-11 PET/CT in a pilot study including 10 patients and additional suspicious PSMA-positive lesions were identified in 4 patients. During the first year of application ^{18}F-JK-PSMA-7 PET/CT detected any PSMA-positive lesions in 84.8% of the patients with biochemical recurrence.

IMPLICATIONS FOR PATIENT CARE: We observed an improved detection rate of ^{18}F-JK-PSMA-7 compared to ^{68}Ga-PSMA-11 in a few selected patients with PSMA-positive lesions in small lymph nodes.

REFERENCES

1. Artibani W, Porcaro AB, De Marco V, Cerruto MA, Siracusano S. Management of biochemical recurrence after primary curative treatment for prostate cancer: a review. *Urol Int.* 2018;100:251-262.

2. Han S, Woo S, Kim YJ, Suh CH. Impact of (68)Ga-PSMA PET on the management of patients with prostate cancer: a systematic review and meta-analysis. *Eur Urol.* 2018;74:179-190.

3. Afshar-Oromieh A, Avtzi E, Giesel FL, et al. The diagnostic value of PET/CT imaging with the (68)Ga-labelled PSMA ligand HBED-CC in the diagnosis of recurrent prostate cancer. *Eur J Nucl Med Mol Imaging.* 2015;42:197-209.

4. Eiber M, Maurer T, Souvatzoglou M, et al. Evaluation of hybrid (68)Ga-PSMA ligand PET/CT in 248 patients with biochemical recurrence after radical prostatectomy. *J Nucl Med.* 2015;56:668-674.

5. Bluemel C, Krebs M, Polat B, et al. 68Ga-PSMA-PET/CT in patients with biochemical prostate cancer recurrence and negative 18F-choline-PET/CT. *Clin Nucl Med.* 2016;41:515-521.

6. Szabo Z, Mena E, Rowe SP, et al. Initial evaluation of [(18)F]DCFPyL for prostate-specific membrane antigen (PSMA)-targeted PET imaging of prostate cancer. *Mol Imaging Biol.* 2015;17:565-574.

7. Dietlein M, Kobe C, Kuhnert G, et al. Comparison of [(18)F]DCFPyL and [(68)Ga]Ga-PSMA-HBED-CC for PSMA-PET imaging in patients with relapsed prostate cancer. *Mol Imaging Biol.* 2015;17:575-584.

8. Giesel FL, Hadaschik B, Cardinale J, et al. F-19 labelled PSMA-1007: biodistribution, radiation dosimetry and histopathological validation of tumor lesions in prostate cancer patients. *Eur J Nucl Med Mol Imaging.* 2017;44:678-688.

9. Rahbar K, Afshar-Oromieh A, Seifert R, et al. Diagnostic performance of ^{18}F-PSMA-1007 PET/CT in patients with biochemical recurrent prostate cancer. *Eur J Nucl Med Mol Imaging.* 2018;45:2055-2061.

10. O'Keefe DS, Su SL, Bacich DJ, et al. Mapping, genomic organization and promoter analysis of the human prostate-specific membrane antigen gene. *Biochem Biophys Acta.* 1998;1443:113-127.

11. O'Keefe DS, Bacich DJ, Heston WD. Comparative analysis of prostate-specific membrane antigen (PSMA) versus a prostate-specific membrane antigen-like gene. *Prostate.* 2004;58:200-210.

12. Afshar-Oromieh A, Debus N, Uhrig M, et al. Impact of long-term androgen deprivation therapy on PSMA ligand PET/CT in patients with castration-sensitive prostate cancer. *Eur J Nucl Med Mol Imaging.* 2018;45:2045-2054.

13. Armstrong IS, Kelly MD, Williams HA, Matthews JC. Impact of point spread function modelling and time of flight on FDG uptake measurements in lung lesions using alternative filtering strategies. *EJNMMI Phys.* 2014;1:99.

14. Jacobson O, Kiesewetter DO, Chen X. Fluorine-18 radiochemistry, labeling strategies and synthetic routes. *Bioconjug Chem.* 2015;26:1-18.

15. Banerjee SR, Pullambhatla M, Byun Y, et al. 68Ga-labeled inhibitors of prostate-specific membrane antigen (PSMA) for imaging prostate cancer. *J Med Chem.* 2010;53:5333-5341.

16. Berry DJ, Ma Y, Ballinger JR, et al. Efficient bifunctional gallium-68 chelators for positron emission tomography: tris(hydroxypyridinone) ligands. *Chem Commun (Camb).* 2011;47:7068-7070.

17. Chen Y, Pullambhatla M, Foss CA, et al. 2-(3-{1-Carboxy-5-[(6-[18F]fluoro-pyridine-3-carbonyl)-amino]-pentyl}-ureido)-pen tanedioic acid, [18F]DCFPyL, a PSMA-based PET imaging agent for prostate cancer. *Clin Cancer Res.* 2011;17:7645-7653.

18. Dietlein F, Kobe C, Neubauer S, et al. PSA-stratified performance of (18)F- and (68)Ga-PSMA PET in patients with biochemical recurrence of prostate cancer. *J Nucl Med.* 2017;58:947-952.

19. Gorin MA, Rowe SP, Patel HD, et al. Prostate specific membrane antigen targeted (18)F-DCFPyL positron emission tomography/computerized tomography for the preoperative staging of high risk prostate cancer: results of a prospective, phase II, single center study. *J Urol.* 2018;199:126-132.

20. Bouvet V, Wuest M, Jans HS, et al. Automated synthesis of [(18)F]DCFPyL via direct radiofluorination and validation in preclinical prostate cancer models. *EJNMMI Res.* 2016;6:40.

21. Ravert HT, Holt DP, Chen Y, et al. An improved synthesis of the radiolabeled prostate-specific membrane antigen inhibitor, [(18) F]DCFPyL. *J Labelled Comp Radiopharm.* 2016;59:439-450.

22. Robu S, Schmidt A, Eiber M, et al. Synthesis and preclinical evaluation of novel (18)F-labeled Glu-urea-Glu-based PSMA inhibitors for prostate cancer imaging: a comparison with (18)F-DCFPyl and (18)F-PSMA-1007. *EJNMMI Res.* 2018;8:30.

23. Zlatopolskiy BD, Endepols H, Krapf P, et al. Discovery of ^{18}F-JK-PSMA-7, a novel PET-probe for the detection of small PSMA positive lesions. *J Nucl Med.* 2019;60:817-823.

24. Wondergem M, van der Zant FM, Vlottes PW, Knol RJJ. Effects of fasting on ^{18}F-DCFPyL uptake in protate cancer lesions and tissues with known high physiologic uptake. *J Nucl Med.* 2018;59:1081-1084.

25. Schmuck S, Nordlohne S, von Klot CA, et al. Comparison of standard and delayed imaging to improve the detection rate of [(68)Ga]PSMA I&T PET/CT in patients with biochemical recurrence or prostate-specific antigen persistence after primary therapy for prostate cancer. *Eur J Nucl Med Mol Imaging.* 2017;44:960-968.

26. Afshar-Oromieh A, Sattler LP, Mier W, et al. The clinical impact of additional late PET/CT imaging with (68)Ga-PSMA-11 (HBED-CC) in the diagnosis of prostate cancer. *J Nucl Med.* 2017;58:750-755.

27. Derlin T, Weiberg D, von Klot C, et al. (68)Ga-PSMA I&T PET/CT for assessment of prostate cancer: evaluation of image quality after forced diuresis and delayed imaging. *Eur Radiol.* 2016;26:4345-4353.

28. Hohberg M, Kobe C, Täger P, et al. Combined early and late [^{68}Ga]Ga-PSMA-HBED-CC PET scans improve lesion detectability in biochemical recurrence of prostate cancer with low PSA levels. *Mol Imaging Biol.* 2019;21:558-566.

29. Hohberg M, Dietlein M, Kobe C, et al. Biodistribution and radiation dosimetry of the novel ^{18}F-labeled prostate-specific membrane antigen-ligand PSMA-7 for PET/CT in prostate cancer patients [abstract]. *J Nucl Med.* 2018;59(Suppl 1):88.

30. Eiber M, Herrmann K, Calais J, et al. Prostate cancer molecular imaging standardized evaluation (PROMISE): Proposed miTNM classification for the interpretation of PSMA-ligand PET/CT. *J Nucl Med.* 2018;59:469-478.

31. Rowe SP, Pienta KJ, Pomper MG, Gorin MA. Proposal for a structured reporting system for prostate-specific membrane antigen-targeted PET imaging: PSMA-RADS version 1.0. *J Nucl Med* 2018;59:479-485.

32. Eder M, Schafer M, Bauder-Wust U, et al. 68Ga-complex lipophilicity and the targeting property of a urea-based PSMA inhibitor for PET imaging. *Bioconjug Chem.* 2012;23:688-697.

33. Schafer M, Bauder-Wust U, Leotta K, et al. A dimerized urea-based inhibitor of the prostate-specific membrane antigen for 68Ga-PET imaging of prostate cancer. *EJNMMI Res.* 2012;2:23.

34. Hammes J, Hohberg M, Täger P, et al. Uptake in non-affected bone tissue does not differ between [18F]-DCFPyL and [68Ga]-HBED-CC PSMA PET/CT. *PLOS ONE.* 2018;13:e0209613.

35. Mannweiler S, Amersdorfer P, Trajanoski S, Terrett JA, King D, Mehes G. Heterogeneity of prostate-specific membrane antigen (PSMA) expression in prostate carcinoma with distant metastasis. *Pathol Oncol Res.* 2009;15:167-172.

36. Fendler WP, Eiber M, Beheshti M, et al. ^{68}Ga-PSMA PET/CT: Joint EANM and SNMMI procedure guideline for prostate cancer imaging: version 1.0. *Eur J Nucl Med Mol Imaging.* 2017;44:1014-1024.

37. Rauscher I, Fendler WP, Hope T, et al. Image quality and lesion detectability using different simulated activities of 68Ga-PSMA.11 [abstract]. *Nuklearmedizin.* 2019;58:150-151.
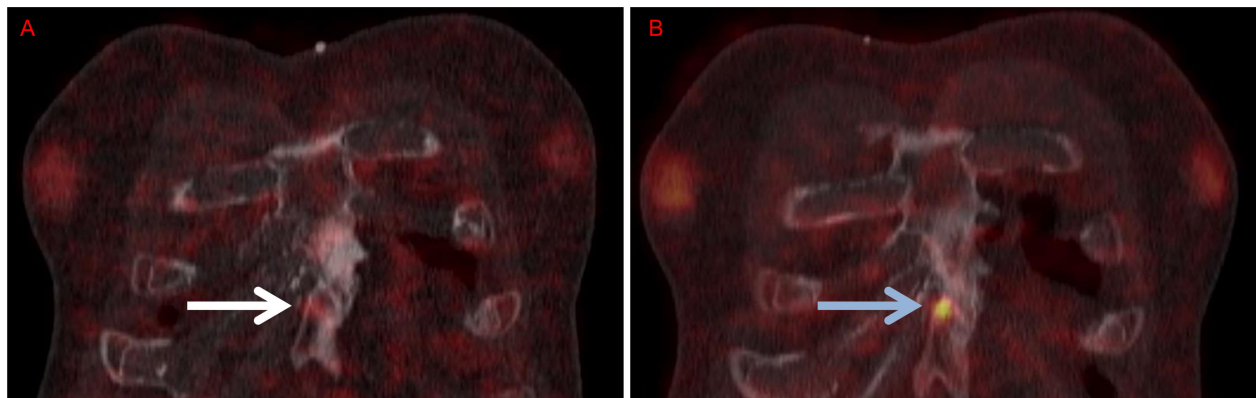
FIGURE 1. (A) ^{68}Ga-PSMA-11 PET/CT on the left and (B) ^{18}F-JK-PSMA-7 PET/CT on the right of patient no. 1. Beside the concordant PSMA-positive tissue within the irradiated prostate (not shown) the patient had previously proven bone metastases, showing positive in the sternum on the ^{18}F-JK-PSMA-7 scan (blue arrow on B), but faintly positive on the ^{68}Ga-PSMA-11 scan (white arrow on A).
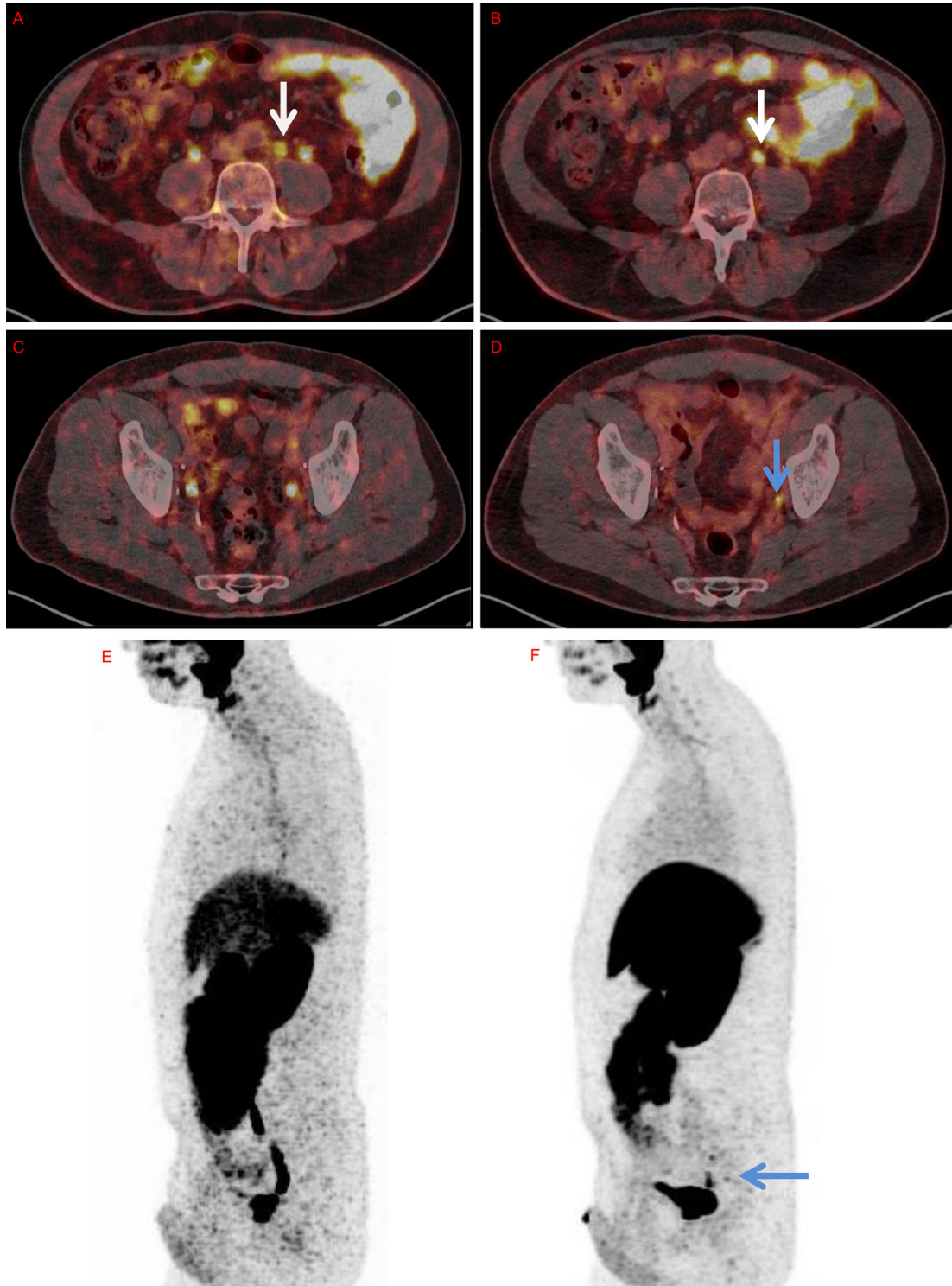
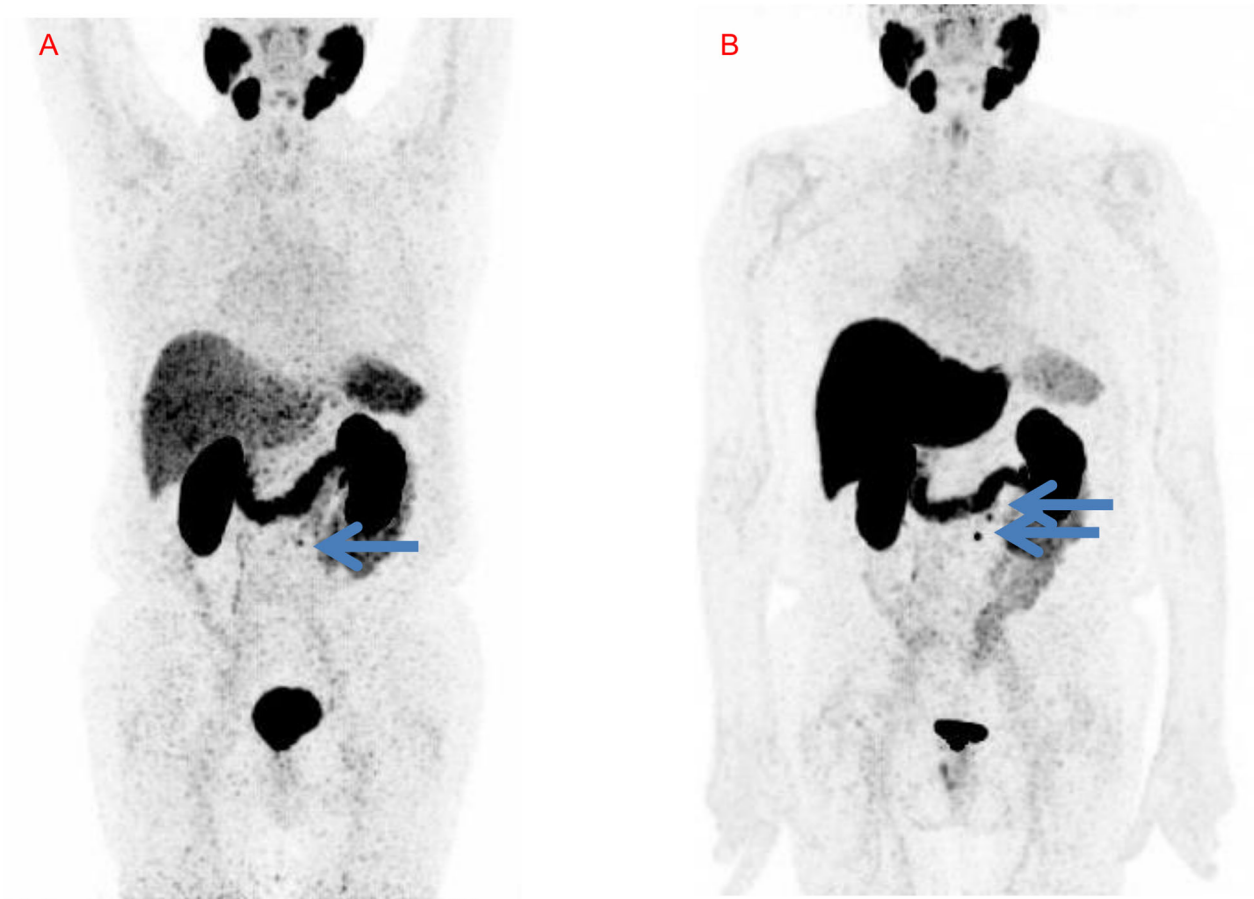**FIGURE 2**. (A,C,E) ^{68}Ga-PSMA-11 PET/CT on the left and (B,D,F) ^{18}F-JK-PSMA-7 PET/CT on the right of patient no. 2. Besides the concordant PSMA-positive lymph node on the left near the bifurcation (white arrows on A and B), ^{18}F-JK-PSMA-7 in this patient revealed a small PSMA-positive left iliac caudal lymph node dorsal to the ureter (blue arrows on D and F).
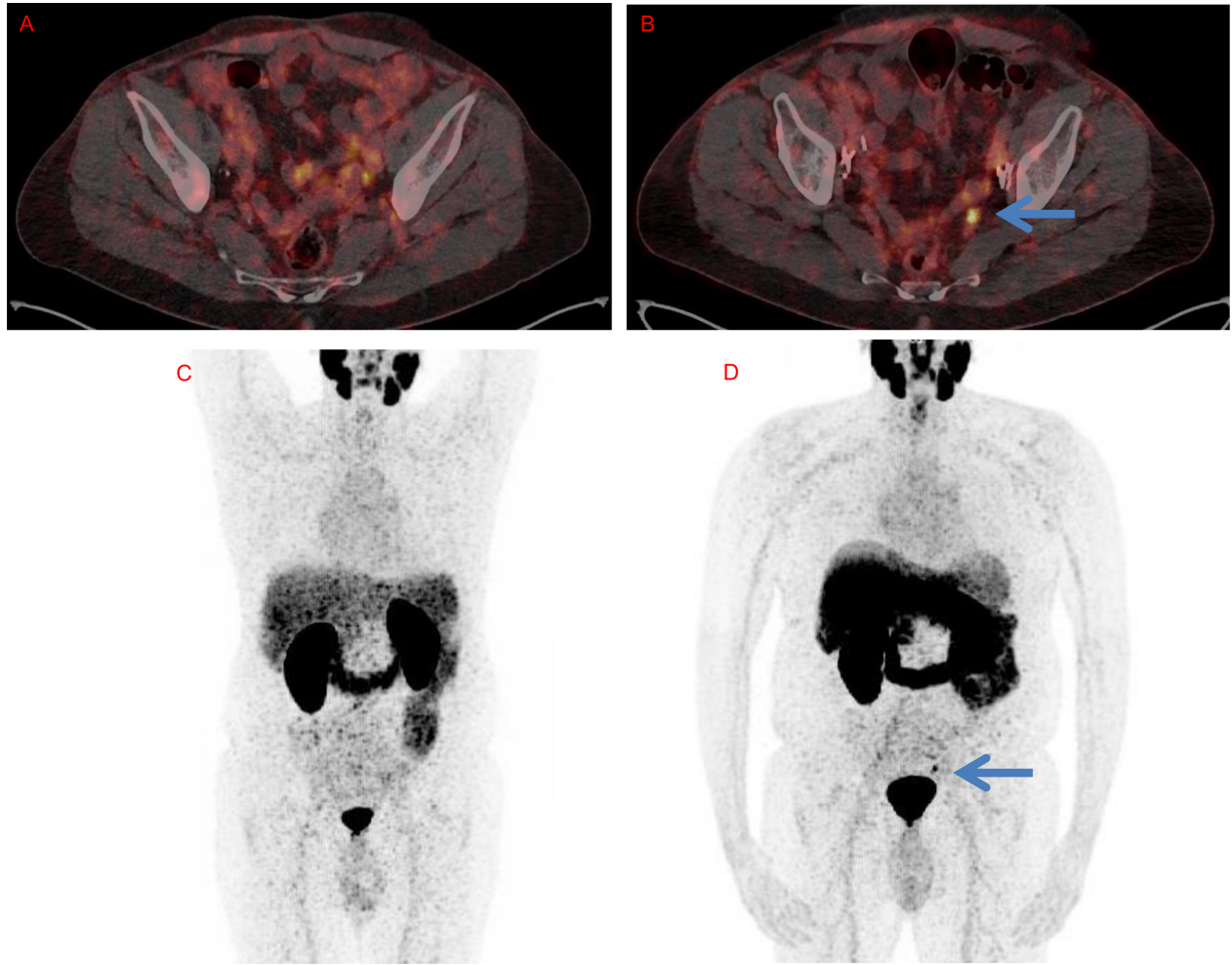
FIGURE 3. (A,C) ^{68}Ga-PSMA-11 PET/CT on the left and (B,D) ^{18}F-JK-PSMA-7 PET/CT on the right of patient no. 4. The PSMA-positive left iliac lymph node was visible on ^{18}F-JK-PSMA-7 PET/CT (blue arrows on B and D).

FIGURE 4. (A) 68Ga-PSMA-11 PET/CT on the left, and (B) 18F-JK-PSMA-7 PET/CT on the right of patient no. 7. The 68Ga-PSMA-11 PET/CT revealed only one PSMA-positive retroperitoneal para-aortal lymph node (blue arrow on A), whereas the 18F-JK-PSMA-7 PET/CT showed 2 PSMA-positive retroperitoneal lymph nodes (blue arrows on B) on the MIP scan (MIP, maximal intensity projection).

patient no.	age (y)	PSA (ng/ml)	indication Gleason score	^{68}Ga dosage ^{18}F dosage (MBq)	local PSMA +	nodal PSMA +	distant PSMA +	therapeutic consequence	verification
1 ^{68}Ga-PSMA ^{18}F-JK-PSMA	76	1.48 with ADT	Taking Bicalutamid. Intensification of ADT? 4+4	160 363	1 1	0 0	0 1	Salvage-RT. Bicalutamid as before without GnRH analoga.	PSA-decrease to 0.23 ng/ml. M osseous confirmed by previous PET/CT.
2 ^{68}Ga-PSMA ^{18}F-JK-PSMA	67	0.7	BCR after prostatectomy 4+3	172 355	0 0	1 left iliac 2 left iliac	0 0	RT of the upper left iliac LN	PSA decrease to 0.5 ng/ml 4 months after RT without ADT. After 10 months PSA 0.6 ng/ml.
3 ^{68}Ga-PSMA ^{18}F-JK-PSMA	66	1.03	BCR after prostatectomy and radiotherapy 3+4	168 347	0 0	(1) retroperitoneal 0	0 0	Wait and see. ^{68}Ga PSMA PET/CT interpreted as unspecific. No indication for LAD or RT	PSA 1.06 ng/ml after 6 months
4 ^{68}Ga-PSMA ^{18}F-JK-PSMA	74	1.1	BCR after prostatectomy 3+4	134 350	0 0	0 1 left iliac	0 0	LAD. After progression (PSA, PET/CT) RT of LN area	LN not confirmed by histology (0/4). PSA increase to 2.6 ng/ml after 8 months, progression proven by external ^{68}Ga-PSMA-11 PET/CT (2 PSMA-positive LN left iliac)
5 ^{68}Ga-PSMA ^{18}F-JK-PSMA	63	4.7	BCR after prostatectomy 4+3	157 329	1 1	0 0	0 0	Salvage-RT of the prostate field	PSA decrease to 0.57 ng/ml
7 ^{68}Ga-PSMA ^{18}F-JK-PSMA	52	14.9	BCR after prostatectomy and radiotherapy 3+3	152 370	0 0	(2) mediastinal 0	0 0	^{68}Ga PSMA PET/CT interpreted as unspecific. No indication for RT of mediastinum	PSMA-negative osteosclerotic bone metastases, detected 9 months later by ^{68}Ga-PSMA PET/CT
8 [^{68}Ga]PSMA [^{18}F]PSMA	73	0.8	BCR after prostatectomy 4+3	129 371	0 0	1 retroperitoneal 3 retroperitoneal	0 0	Further PSA increase to 1.13 ng/ml. Then RT of retroperitoneal LN area.	PSA decrease to 0.42 ng/ml 4 months after RT without ADT. ^{18}F-PSMA PET/CT (346 MBq) follow-up confirmed at least 2 retroperitoneal PSMA-positive LN.
9 ^{68}Ga-PSMA ^{18}F-JK-PSMA	74	1.017	BCR after prostatectomy 3+4	153 379	0 0	0 0	0 0	Without any therapy PSA 0.7 ng/ml after 6 months and 1,2 ng/ml after 8 months	n.a.
10 ^{68}Ga-PSMA ^{18}F-JK-PSMA	59	0.51	BCR after prostatectomy 4+3	110 345	0 0	0 0	0 0	RT of prostate fossa with regard to R1 and negative PSMA PET scans.	PSA decrease to 0.4 ng/ml after 8 months without ADT
11 ^{68}Ga-PSMA ^{18}F-JK-PSMA	69	0.46	BCR after prostatectomy 4+3	76 370	1 1	0 0	0 0	RT of prostate fossa (standard field)	

TABLE 1. Patient characteristics and localization of the pathological PSMA uptake detected by ^{68}Ga-PSMA-11 PET/CT and ^{18}F-JK-PSMA-7 PET/CT in the initial cohort of 10 patients. Patient No. 6 did not receive ^{68}Ga-PSMA-11 PET/CT and was not included in our direct comparison. ADT, androgen deprivation therapy; BCR, biochemical recurrence; GnRH, gonadotropin releasing hormone; LAD, lymphadenectomy; LN, lymph node; n.a., not available; PSMA, prostate-specific membrane antigen; S-LAD, salvage lymphadenectomy; S-RT, salvage radiotherapy; RT, radiotherapy; ^{68}Ga-PSMA, ^{68}Ga-PSMA-11 PET/CT; ^{18}F-PSMA, ^{18}F-JK-PSMA-7 PET/CT.

Indication for ^{18}F-JK-PSMA-7 PET/CT	PSMA neg.	PSMA pos.	T+	N+	M+	T+N+	T+M+	N+M+	T+N+M+
BCR or PSA increase after PE ± RT (all)	9	40	10	19	4	1	4	2	
PSA < 0.2 µg/l	1	1		1 (oligo 1)					
BCR, PSA 0.2 – 0.49 µg/l	4	5	2	3 (oligo 1)					
BCR, PSA 0.5 – 1.99 µg/l	2	14	2	7 (oligo 6)	3	1	1		
BCR, PSA ≥ 2.0 µg/l	2	20	6	8 (oligo 2)	1		3	2	
BCR or PSA increase after RT (all)	7	19	8	3	3	2	1	1	1
Δ PSA < 2.0 µg/l	6	3	1	1 (oligo 1)	1				
BCR, Δ PSA ≥ 2.0 µg/l	1	16	7	2	2	2 (oligo 1)	1	1	1

TABLE 2. Results of ^{18}F-JK-PSMA-7 PET/CT in 75 patients with BCR, specified by the initial therapy, and the PSA level. The BCR was defined by a PSA level of ≥ 0.2 µg/l after prostatectomy or by an increase in PSA level of ≥ 2.0 µg/l above nadir after radiotherapy. Some patients were sent to ^{18}F-JK-PSMA-7 PET/CT before these criteria were fulfilled and were separately reported. Abbreviations: BCR, biochemical recurrence; oligo, oligo-metastasized (here: ≤ 3 PSMA-positive lymph nodes); PE, prostatectomy; PSMA, prostate specific membrane antigen; RT radiotherapy; T+, PSMA-positive tissue within the prostate fossa; N+, PSMA-positive lymph node; M+, PSMA-positive lesion in the bone, lung or liver